Meta-Learned Regional Initialization of Control Filters for Headphone Active Noise Control

Ziyi Yang*, Zhengding Luo*, Dongyuan Shi†, Junwei Ji*, Boxiang Wang*, Haowen Li*,
Qirui Huang* and Woon-Seng Gan*
* Nanyang Technological University, Singapore
† Northwestern Polytechnical University, China
E-mail: {ziyi016, luoz0021}@e.ntu.edu.sg, dongyuan.shi@nwpu.edu.cn, {junwei002, boxiang001}@e.ntu.edu.sg,
haowen.li@ntu.edu.sg, huang.qirui@ieee.org, ewsgan@ntu.edu.sg

***Abstract*—This paper proposes a regional meta-initialization framework for binaural headphone active noise control (ANC), based on the modified Model-Agnostic Meta-Learning (MAML) method. By leveraging multiple spatially distributed training tasks, the framework learns a shared initialization of the control filter that facilitates faster convergence and more effective early-stage noise attenuation under changing acoustic paths. The framework is evaluated on a measured headphone ANC path dataset covering 24 azimuth-distance configurations. Simulation results demonstrate that the meta-initialized control filters outperform zero and single-location pre-trained initializations in early-stage noise suppression and convergence speed under unseen noise source positions. The findings provide preliminary validation that meta-initialization enhances ANC performance across diverse real-world acoustic paths.**

I. Introduction

Active noise control (ANC) has become a widely adopted technique and has received increasing attention in recent years for protecting individuals from the effects of environmental noise [1]–[6], particularly in low-frequency ranges where passive methods are less effective [7]. It operates by generating anti-phase signals that destructively interfere with incoming disturbance, enabling real-time noise attenuation. Based on the stage of control intervention, ANC systems can be implemented at noise source, transmission path, or receiver-end [8]. Receiver-end control is the most commonly employed in commercial products due to its adaptability to dynamic acoustic environments and user-specific conditions. Headphone ANC represents a typical receiver-end configuration, where microphones and loudspeakers are integrated near the ears to enable localized and real-time noise cancellation [9], [10].

Commercial headphones predominantly use feedforward ANC, where external microphones capture the disturbance ahead of the ear. This structure provides effective broadband attenuation but its performance depends on source direction and motion, since contralateral incidence can break causality and reduce prediction quality [11]–[13]. Binaural architectures coordinate the two ears and improve robustness to spatial variation [14], [15], yet they still rely on online adaptation. In practice the FxLMS controller is often initialized at or near zero, which yields slow start-up convergence. Heuristics such as step-size scheduling and frequency-domain variants can speed up learning but frequently trade steady-state accuracy for speed and transfer poorly across spatial changes [16]–[18]. Data-driven fixed-filter designs provide an immediate response [19], [20], but the filters are tied to the training conditions and degrade at unseen positions. These limitations motivate learning a shared initialization that is robust across spatial tasks and adapts quickly when the source direction or distance changes.

While binaural configuration extends headphone ANC system's spatial coverage to directional variations, it remains constrained by limited adaptation speed under noise direction shifts. Conventional adaptive algorithms, such as the filtered-x least mean squares (FxLMS), rely on zero or random initialization of control filters and require a certain iterations to reach steady-state performance. Various efforts have been made to accelerate the convergence of FxLMS, like step-size tuning [16], variable step-size algorithms [17], and frequency-domain approaches [18]. However, these methods often involve trade-offs between convergence speed, steady-state accuracy, and computational complexity, and their generalizability across diverse spatial scenarios remains limited. To address the adaptation latency of FxLMS-based methods and capture nonlinear relationships, deep learning-based ANC frameworks have recently been proposed [19]–[21]. Selective fixed-filter ANC selects from pre-trained filters based on noise features [19], [22], while generative fixed-filter ANC employs CNN to generate control filters from noise input [23]. These approaches offer fast response but have limited ability to transfer across unseen acoustic environments.

To overcome the limitations in convergence speed and generalization across varying acoustic environments, Model-Agnostic Meta-Learning (MAML) has been applied to optimize the initialization of control filters [24], [25]. It was demonstrated that MAML enable faster convergence across varying noise types and primary paths, and this is especially beneficial in binaural headphone ANC, where DOA dependency, and slow adaptation remain critical challenges.In this paper, we propose a meta-learned regional initialization framework for binaural headphone ANC, where control filter parameters are initialized via MAML across spatially distributed noise source positions. By optimizing a shared

979-8-3315-7206-8/25/$31.00

initialization over a range of acoustic paths, the proposed method enables rapid adaptation to unseen directional and positional variations, addressing the convergence and generalization challenges of conventional approaches. Experimental evaluations on measured headphone impulse responses demonstrate that our method improves both transient response and spatial robustness across regional noise conditions.

II. Headphone ANC System and Dataset Setup

A. Binaural FxLMS based ANC algorithm

In headphone-based active noise control (ANC), the binaural FxLMS algorithm aims to minimize the acoustic disturbance at both ears by jointly adapting the control filters using spatially distributed reference information. Compared to independent bilateral ANC configurations, the binaural setup allows for interaural signal coupling, which enhances spatial awareness and noise reduction performance across varying sound incidence angles.

As depicted in Fig. 1, the system inputed with 2 reference microphones from each earcup, acquiring the reference signals denoted as x_L and x_R, respectively. These signals capture the ambient sound field as received near the left and right ears, and serve as the inputs to the ANC controller. The control signals y_L and y_R are generated by adaptive filters $\mathbf{w}_L$ and $\mathbf{w}_R$ and fed to the loudspeakers embedded in each earcup. The estimated secondary paths $\hat{\mathbf{s}}_L$ and $\hat{\mathbf{s}}_R$ are used to filter the reference signals, producing $\mathbf{x}_{rL}(n)$ and $\mathbf{x}_{rR}(n)$ as inputs to the LMS update.

In the binaural configuration, the adaptation of each control filter uses both ipsilateral and contralateral reference signals, filtered through the corresponding secondary path estimates. For details, the update of the control filter is based on the error signal $e(n)$ and the filtered reference vector:

$$\mathbf{x}_{rL}(n) = \left[\hat{\mathbf{s}}_L^{\mathrm{T}}(n) * \mathbf{x}_L^{\mathrm{T}}(n),\ \hat{\mathbf{s}}_L^{\mathrm{T}}(n) * \mathbf{x}_R^{\mathrm{T}}(n)\right]^{\mathrm{T}} \tag{1}$$

$$\mathbf{x}_{rR}(n) = \left[\hat{\mathbf{s}}_R^{\mathrm{T}}(n) * \mathbf{x}_L^{\mathrm{T}}(n),\ \hat{\mathbf{s}}_R^{\mathrm{T}}(n) * \mathbf{x}_R^{\mathrm{T}}(n)\right]^{\mathrm{T}} \tag{2}$$

where $\mathbf{x}_L(n) = [x_L(n), x_L(n-1), \ldots, x_L(n-N+1)]^{\mathrm{T}}$ and $\mathbf{x}_R(n) = [x_R(n), x_R(n-1), \ldots, x_R(n-N+1)]^{\mathrm{T}}$ are the reference signal vectors of length N for the left and right channels, respectively.

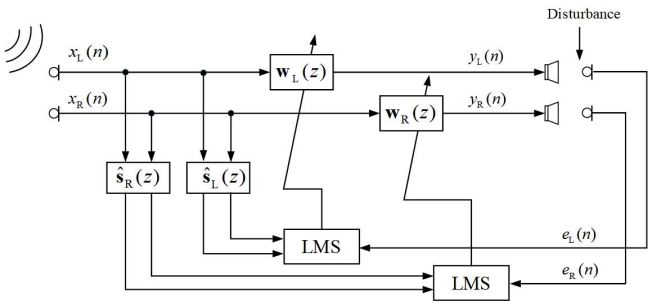

Fig. 1. Block diagram of binaural FxLMS-based headphone ANC system

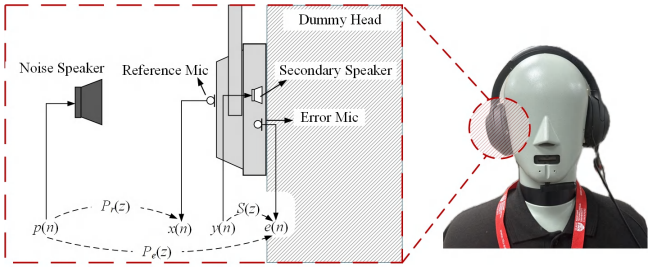

Fig. 2. Measurement setup for headphone ANC path recording.

The adaptive update rule is:

$$\mathbf{w}_i(n+1) = \mathbf{w}_i(n) + \mu\, e_i(n)\, \mathbf{x}_{ri}(n) \tag{3}$$

where μ is the learning rate and and $i \in \{L, R\}$ denotes the channel index, corresponding to the left and right ears, respectively.

The binaural FxLMS algorithm updates both control filters using reference signals from both ears, enabling spatially aware ANC processing in headphone systems.

B. Measurement Dataset

The measurement dataset was collected using a headphone-mounted ANC system based on a dummy head (B&K 4128-C). The setup is illustrated in Fig. 2, where broadband noise is emitted by a loudspeaker placed at varying positions in front of the subject. Reference microphones are mounted on the outer shell of the headphones, while error microphones are embedded near the ear canal. The measured signals were digitized and recorded using a dSPACE DS3604 system at a sampling rate of 48 kHz. Based on the recorded signals, the primary path models $P_r(z)$ and $P_e(z)$, as well as the secondary path $S(z)$, were identified using system identification techniques.

To capture spatial variation in primary acoustic paths, we performed controlled recordings in an acoustic booth treated with sound absorption to suppress reflections and reverberations, as shown in Fig. 3A. A single loudspeaker served as the noise source, and the dummy head was rotated horizontally to simulate noise incidence from different angles. The measurement covered 8 azimuthal directions (0° to 360° at 45°

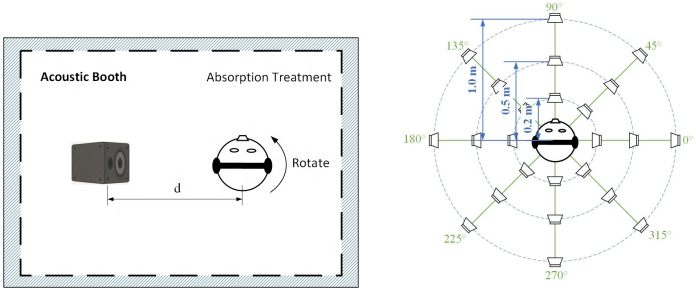

Fig. 3. Experimental measurement setup for headphone ANC path. (a) acoustic booth layout; (b) noise source positions covering 8 azimuths and 3 distances.

resolution) and 3 radial distances (0.2m, 0.5m, and 1.0m), as depicted in Fig.3(b).

This results in a total of 24 unique spatial configurations for each ear, enabling the evaluation of spatial generalization performance under various sound source directions and distances.

III. Modified Model-Agnostic Meta-Learning for Control Filter Initialization

A. Model-Agnostic Meta-Learning

Unlike conventional training that optimizes a single model on a specific dataset, meta-learning often described as learning to learn[26], trains a learner to adapt quickly across a distribution of related tasks rather than optimizing a single model on a specific dataset. Each task supplies two small splits: a support set for a few adaptation steps and a query set for evaluating the adapted model[27]. The aim is to learn meta-parameters such as an initialization or an update rule that, after this short within-task adaptation, minimize the expected loss on the query sets across tasks. This two-level optimization is well suited to settings where deployment conditions change and only short data segments are available per condition[28], [29].

Within this meta-learning setup, model-agnostic meta-learning provides a gradient-based instantiation[30]. It learns a shared initialization $\mathbf{\Phi}$ so that tasks $\tau \sim p(\tau)$ can be solved with a few gradient steps and little data. For each task τ, we set $\mathbf{w}_\tau^{(0)} = \mathbf{\Phi}$ and take K gradient updates on its support set to obtain the adapted parameters $\mathbf{w}_\tau^{(K)}$. The outer objective then updates $\mathbf{\Phi}$ to minimize the expected validation loss after adaptation:

$$\mathbf{\Phi}^\star = \arg\min_{\mathbf{\Phi}} \mathbb{E}_{\tau\sim p(\tau)}\big[\mathcal{L}_{\text{val}}(\mathbf{w}_\tau^{(K)})\big]. \tag{4}$$

where $\mathcal{L}_{\text{val}}$ is the loss function that evaluates the loss of $\mathbf{w}_\tau^{(K)}$ on the task's query set and its exact form is application dependent. Variants that approximate or reparameterize the meta-gradient include first-order methods [31] and implicit-gradient approaches [32].

B. MAML initialization for ANC

In headphone ANC the operating condition is defined by the source direction and distance, with the measured secondary path held fixed. We treat each such condition as one task. For every task we generate independent white-noise audio segments; some segments form the support set for K inner updates and the remaining segments form the query set for validation. The inner loop follows the FxLMS update with filtered references. The outer objective then updates the initialization $\mathbf{\Phi}$ to reduce the average query error across tasks. We use a first-order meta-gradient for the outer update to avoid backpropagating through the FxLMS recursion [24]. The details of each step are as follows:

Algorithm 1 Pseudo code of the modified MAML algorithm for multi-reference ANC

Input: Reference signal track $\mathbf{x}_c$, correspond disturbance signal track $\mathbf{d}_c$, secondary-path model $\mathbf{s}$
Initialized: Meta control filter $\mathbf{\Phi}$, total epochs K, step size μ, forgetting factor λ, meta-learning rate α
/* Across-task loop */
for epoch $i = 1$ to K **do**
  /* Within-task training */
  Sampling $\mathbf{x}_j(n)$ from $\mathbf{x}_c$, $d(n)$ from $\mathbf{d}_c$, and get correspond filtered references $\mathbf{x}'_j(n)$
  Initialize filter $\mathbf{w} \leftarrow \mathbf{\Phi}$
  $e(n) = d(n) - \sum_{j=1}^{J} \mathbf{x}_j'^{\mathrm{T}}(n)\,\mathbf{w}_j$
  for $j = 1$ to J **do**
    $\mathbf{w}_j \leftarrow \mathbf{w}_j + \mu\, e(n)\, \mathbf{x}'_j(n)$
  end for
  /* Within-task testing */
  for $t = 0$ to $N-1$ **do**
    $e^\dagger(n-t) \leftarrow d(n-t) - \sum_{j=1}^{J} \mathbf{w}_j^T \mathbf{x}_j(n-t)$
  end for
  /* MAML-update */
  for $j = 1$ to J **do**
    $\Delta\Phi_j \mathrel{+}= \sum_{t=0}^{N-1} \lambda^t\, e^\dagger(n-t)\, \mathbf{x}_j(n-t)$
    $\Phi_j \leftarrow \Phi_j + \alpha\, \Delta\Phi_j, \quad \Delta\Phi_j \leftarrow \mathbf{0}$
  end for
end for

1) Within-task Training: Given a sampled task, we draw a short segment of reference signals $\mathbf{x}_j(n)$ and disturbance $d(n)$ from the training set. Each reference is filtered through an estimated secondary path $\hat{\mathbf{s}}_j$ to generate the filtered input:

$$\mathbf{x}'_j(n) = \hat{\mathbf{s}}_j * \mathbf{x}_j(n). \tag{5}$$

Let the meta-initialized control filter be $\mathbf{\Phi} = [\mathbf{\Phi}_1, \ldots, \mathbf{\Phi}_J]$, which is copied to task-specific filter $\mathbf{w}_j(0) = \mathbf{\Phi}_j$. The error signal at each time n is:

$$e(n) = d(n) - \sum_{j=1}^{J} \mathbf{x}_j'^T(n)\mathbf{w}_j(n). \tag{6}$$

The filter is then updated using the filtered-x LMS rule:

$$\mathbf{w}_j(n{+}1) = \mathbf{w}_j(n) + \mu\, e(n)\, \mathbf{x}'_j(n), \tag{7}$$

where μ is the step size for adaptation.

2) Within-task Testing: After adaptation for N iterations, the updated control filter $\mathbf{w}_j(N)$ is evaluated on a separate test segment from the same task. The post-adaptation error is computed as:

$$e^\dagger(n{-}t) = d(n{-}t) - \sum_{j=1}^{J} \mathbf{w}_j^T \mathbf{x}_j(n{-}t), \quad t = 0, \ldots, N{-}1. \tag{8}$$

3) Meta-update: To update the meta-initialization $\mathbf{\Phi}$, the gradient of the meta-loss is computed. For each reference channel j, we compute:

$$\Delta\mathbf{\Phi}_j = \sum_{t=0}^{N-1} \lambda^t \, e^{\dagger}(n-t)\, \mathbf{x}_j(n-t), \tag{9}$$

where $\lambda \in (0, 1]$ is a temporal forgetting factor emphasizing recent errors. The meta-parameters are updated using gradient descent[30]:

$$\mathbf{\Phi}_j \leftarrow \mathbf{\Phi}_j + \alpha\, \Delta\mathbf{\Phi}_j, \tag{10}$$

where α is the meta-learning rate.

4) Across-task Iteration: In the outer loop, K epochs are executed. At each epoch, one meta-training task (a direction–distance configuration) is drawn uniformly. Fresh support and query segments are generated from independent band-limited noise, while the secondary path model is held fixed. The task is processed as follows: initialize the task filter by $\mathbf{w} \leftarrow \mathbf{\Phi}$; perform within-task training using the FxLMS updates; evaluate the post-adaptation error on the query segment; compute the channel-wise meta-gradient via (9); and immediately update the meta-parameters using (10). The accumulator is then reset, $\Delta\mathbf{\Phi} \leftarrow \mathbf{0}$, and the next epoch proceeds with a newly sampled task.

IV. Simulations and Analysis

A. Experimental Setup

In this section, we evaluate the spatial generalization and online adaptation based on the measured headphone ANC dataset described in Section II. The spatial layout of source positions is shown in Fig. 4. Six positions (marked as blue) serve as meta-training tasks for MAML, and a single-location FxLMS baseline is trained at the position (marked as yellow) near T1. Three unseen test positions (marked as red, T1–T3) cover distinct directions and distances.

For each spatial task, independent band-limited white-noise segments (200–700 Hz) were generated. Support segments were used for within-task updates and query segments for validation. The secondary path was fixed to the measured model. Unless stated otherwise, the metric is noise reduction in dB relative to the original sound power level (SWL). For adaptation experiments, FxLMS was run for 5 s with a common step size μ=0.001; adaptation begins at 0.5 s.

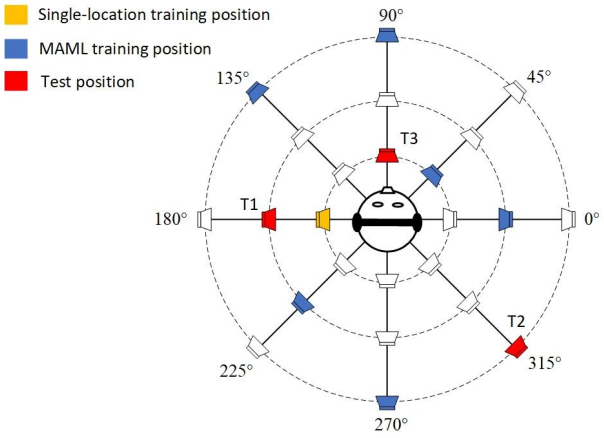

Fig. 4. Selected primary source positions used for training and testing

TABLE I
NOISE REDUCTION COMPARISON OF INITIALIZATION STRATEGIES WITHOUT ADAPTATION

Initialization Strategy	Ear	T1	T2	T3
Zero	**Left / Right**	0.0 dB	0.0 dB	0.0 dB
Single-location	**Left**	5.3 dB	-0.6 dB	2.6 dB
	Right	3.2 dB	-6.6 dB	4.6 dB
MAML-front	**Left**	6.0 dB	6.1 dB	14.8 dB
	Right	5.3 dB	8.1 dB	13.1 dB
MAML-omni	**Left**	9.4 dB	10.4 dB	15.1 dB
	Right	9.3 dB	13.0 dB	12.6 dB

Four initialization schemes were compared:

- **Zero initialization**: all coefficients initialized to zero.
- **Single-location initialization**: FxLMS pre-trained at the yellow position in Fig. 4.
- **MAML-front initialization**: meta-initialization trained on 3 forward-facing positions (45°, 90°, 135°).
- **MAML-omni initialization**: meta-initialization trained on 6 distributed positions (blue in Fig. 4).

B. Initialization-Only Generalization (No Adaptation)

The effect of initialization was isolated by evaluating the 4 strategies at T1–T3 without further adaptation. Table I summarizes the results. Two points can be found. (i) Both meta-initializations offer a stronger starting point than Zero or Single-location at all test positions. MAML-omni reaches 9.4/9.3 dB (left/right) at T1, 10.4/13.0 dB at T2, and 15.1/12.6 dB at T3. MAML-front is consistently weaker than MAML-omni yet clearly better than the baselines, reaching 6.0/5.3 dB at T1, 6.1/8.1 dB at T2, and 14.8/13.1 dB at T3. In contrast, Single-location transfers poorly to T2, with -0.6 dB on the left and -6.6 dB on the right. (ii) The breadth of spatial coverage during meta-training is important. The broader coverage of MAML-omni yields the most consistent gains across directions. At T3, which is locally similar to several training directions, both meta-initializations deliver their largest improvements, indicating that the learned prior captures reusable spatial structure.

C. Online Adaptation and Convergence

Convergence was assessed by running FxLMS from each initialization; Fig. 5 shows mean-square-error trajectories at T1 (180°, 0.5 m), T2 (315°, 1.0 m), and T3 (90°, 0.2 m). Across all cases, **MAML-omni** converges fastest and attains the lowest steady-state error. **Single-location** helps near its training neighborhood (T1) but converges slowly and saturates higher at T2, reflecting directional mismatch. At T3 the largest gains appear for both meta-initializations, consistent with local similarity to several training directions; MAML-omni remains

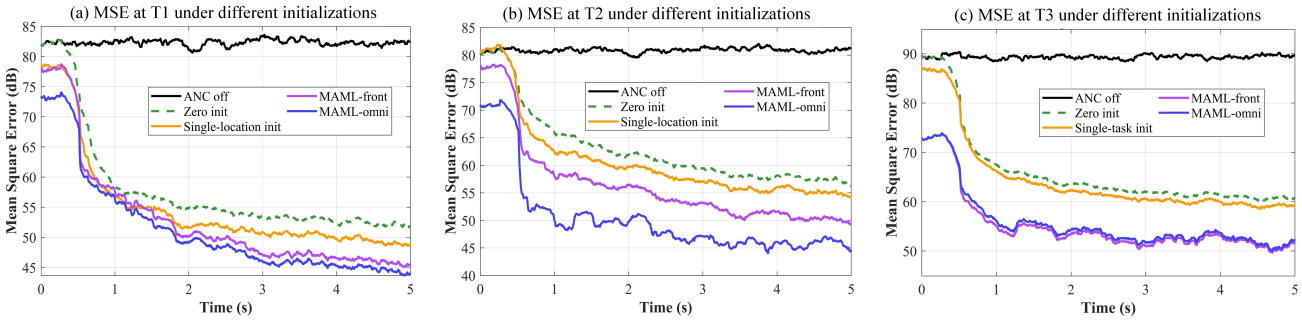

Fig. 5. MSE at left error under different initialization strategies using FxLMS (stepsize = 0.001) at 2 test positions, adaptation begins at 0.5 s. (a) T1 located at 180° and 0.5 m, (b) T2 located at 315° and 1.0 m, and (c) T3 located at 90° and 0.2 m.

best in both transient and final error. A mild decline before 0.5 s stems from the sliding-window MSE and short buffer warm-up of the filtered references, not from weight updates. All runs use the same step size ($\mu = 0.001$); right-ear results follow the same pattern and are omitted for brevity.

D. Discussions

The main strengths are twofold. First, good generalization is obtained at unseen source positions while using only a small number of measured path configurations for training. The meta–initialized filter already reduces error before adaptation and shortens the transient once FxLMS starts, with no extra run-time cost beyond a standard controller. Second, the approach remains compatible with classical ANC practice since only an initialization is learned and the on-line adaptation is still FxLMS, which preserves stability and interpretability.

There are, however, some limitations. Performance depends on how the meta-training positions are chosen and on the spatial coverage they provide. A single shared initialization cannot fully represent multiple, widely separated operating regimes; when the task shifts far in angle or distance, attenuation can drop. The learned prior is also sensitive to secondary-path mismatch and to the excitation band used during training, which restricts high-frequency robustness. Using a sequential first-order outer update reduces cost but increases gradient variance, so the outcome is sensitive to the meta rate, adaptation step size, and forgetting factor. Finally, the dataset measurement was conducted in a controlled booth with a stationary head and band-limited noise, reverberant rooms were not addressed.

V. Conclusions

This paper presents a regional meta-initialization framework for binaural headphone ANC based on Model-Agnostic Meta-Learning. By learning a shared initialization across spatially diverse training tasks, the proposed method enables more effective early-stage control and faster convergence during real-time adaptation. Experimental evaluation on a measured headphone paths dataset confirms that the MAML-initialized controller consistently achieves lower steady-state error and improved spatial generalization compared to zero and single-location initializations. Notably, the framework demonstrates robustness under noise source positions' mismatch, validating its potential for real-world ANC applications where noise source directions vary dynamically. Furthermore, our analysis reveals that the selection of meta-training directions significantly impacts the performance of the initialization. MAML trained on omni-directional positions generalizes better across unseen source locations. Future work will focus on operation in more realistic settings, including reverberant rooms, moving sources, and head motion. Robustness to secondary-path drift and nonstationary noise will be pursued via path perturbation and data augmentation.

References

[1] S. M. Kuo and D. R. Morgan, *Active noise control systems*. Wiley, New York, 1996, vol. 4.

[2] B. Lam, W.-S. Gan, D. Shi, M. Nishimura, and S. Elliott, "Ten questions concerning active noise control in the built environment," *Building and Environment*, vol. 200, p. 107 928, 2021.

[3] J. Zhang, S. J. Elliott, and J. Cheer, "Robust performance of virtual sensing methods for active noise control," *Mechanical Systems and Signal Processing*, vol. 152, p. 107 453, 2021.

[4] Z. Yang, S. Wang, J. Tao, and X. Qiu, "Active control of sound transmission through a floor-level slit," *The Journal of the Acoustical Society of America*, vol. 154, no. 5, pp. 2746–2756, 2023.

[5] T. Li, S. Lian, S. Zhao, J. Lu, and I. S. Burnett, "Distributed active noise control based on an augmented diffusion fxlms algorithm," *IEEE/ACM Transactions on Audio, Speech, and Language Processing*, vol. 31, pp. 1449–1463, 2023.

[6] Z. Luo, H. Ma, D. Shi, and W.-S. Gan, "Gfanc-rl: Reinforcement learning-based generative fixed-filter active noise control," *Neural Networks*, p. 106 687, 2024.

[7] C. H. Hansen, S. D. Snyder, X. Qiu, L. A. Brooks, and D. J. Moreau, *Active control of noise and vibration*. E & Fn Spon London, 1997.

[8] P. A. Nelson and S. J. Elliott, *Active Control of Sound*. Academic Press, 1992.

[9] W.-S. Gan, S. Mitra, and S. M. Kuo, "Adaptive feedback active noise control headset: Implementation, evaluation and its extensions," *IEEE Transactions on Consumer Electronics*, vol. 51, no. 3, pp. 975–982, 2005.

[10] S. M. Kuo, S. Mitra, and W.-S. Gan, "Active noise control system for headphone applications," *IEEE Transactions on Control Systems Technology*, vol. 14, no. 2, pp. 331–335, 2006.

[11] L. Zhang and X. Qiu, "Causality study on a feedforward active noise control headset with different noise coming directions in free field," *Applied Acoustics*, vol. 80, pp. 36–44, 2014.

[12] S. Liebich, J.-G. Richter, J. Fabry, C. Durand, J. Fels, and P. Jax, "Direction-of-arrival dependency of active noise cancellation headphones," in *Noise Control and Acoustics Division Conference*, American Society of Mechanical Engineers, vol. 51425, 2018, V001T08A003.

[13] J. Cheer, V. Patel, and S. Fontana, "The application of a multi-reference control strategy to noise cancelling headphones," *The Journal of the Acoustical Society of America*, vol. 145, no. 5, pp. 3095–3103, 2019. DOI: 10.1121/1.5109394.

[14] B. Cornelis, S. Doclo, T. Van dan Bogaert, M. Moonen, and J. Wouters, "Theoretical analysis of binaural multimicrophone noise reduction techniques," *IEEE Transactions on Audio, Speech, and Language Processing*, vol. 18, no. 2, pp. 342–355, 2009.

[15] R. Serizel, M. Moonen, J. Wouters, and S. H. Jensen, "Binaural integrated active noise control and noise reduction in hearing aids," *IEEE Transactions on Audio, Speech, and Language Processing*, vol. 21, no. 5, pp. 1113–1118, 2012.

[16] J. Lee and Y. Park, "A step-size control algorithm for the filtered-x lms algorithm," *IEEE Signal Processing Letters*, vol. 7, no. 5, pp. 106–108, 2000. DOI: 10.1109/97.839636.

[17] J. Xu, Y. Zhu, and Q. Gu, "A new variable step-size lms algorithm and its performance analysis," *IEEE Transactions on Signal Processing*, vol. 51, no. 5, pp. 1253–1262, 2003. DOI: 10.1109/TSP.2003.810292.

[18] J.-H. Chang and C. Un, "A modified frequency-domain filtered-x lms algorithm for active noise control," *IEEE Transactions on Speech and Audio Processing*, vol. 11, no. 6, pp. 603–607, 2003. DOI: 10.1109/TSA.2003.819954.

[19] D. Shi, W.-S. Gan, B. Lam, and S. Wen, "Feedforward selective fixed-filter active noise control: Algorithm and implementation," *IEEE/ACM Transactions on Audio, Speech, and Language Processing*, vol. 28, pp. 1479–1492, 2020.

[20] Z. Luo, D. Shi, X. Shen, J. Ji, and W.-S. Gan, "Deep generative fixed-filter active noise control," in *ICASSP 2023-2023 IEEE International Conference on Acoustics, Speech and Signal Processing*, IEEE, 2023, pp. 1–5.

[21] H. Zhang and D. Wang, "Deep anc: A deep learning approach to active noise control," *Neural Networks*, vol. 141, pp. 1–10, 2021.

[22] Z. Luo, D. Shi, and W.-S. Gan, "A hybrid sfanc-fxnlms algorithm for active noise control based on deep learning," *IEEE Signal Processing Letters*, vol. 29, pp. 1102–1106, 2022.

[23] Z. Luo, D. Shi, X. Shen, J. Ji, and W.-S. Gan, "Gfanc-kalman: Generative fixed-filter active noise control with cnn-kalman filtering," *IEEE Signal Processing Letters*, vol. 31, pp. 276–280, 2023.

[24] D. Shi, W.-S. Gan, B. Lam, and K. Ooi, "Fast adaptive active noise control based on modified model-agnostic meta-learning algorithm," *IEEE Signal Processing Letters*, vol. 28, pp. 593–597, 2021.

[25] X. Shen, D. Shi, and W.-S. Gan, "Data-driven method to accelerate convergence of adaptive hybrid active noise control: Two-stage model-agnostic meta-learning," *IEEE Signal Processing Letters*, 2025.

[26] S. Thrun and L. Pratt, "Learning to learn: Introduction and overview," in *Learning to learn*, Springer, 1998, pp. 3–17.

[27] O. Vinyals, C. Blundell, T. Lillicrap, D. Wierstra, *et al.*, "Matching networks for one shot learning," *Advances in neural information processing systems*, vol. 29, 2016.

[28] S. Ravi and H. Larochelle, "Optimization as a model for few-shot learning," in *International conference on learning representations*, 2017.

[29] T. Hospedales, A. Antoniou, P. Micaelli, and A. Storkey, "Meta-learning in neural networks: A survey," *IEEE transactions on pattern analysis and machine intelligence*, vol. 44, no. 9, pp. 5149–5169, 2021.

[30] C. Finn, P. Abbeel, and S. Levine, "Model-agnostic meta-learning for fast adaptation of deep networks," in *International conference on machine learning*, PMLR, 2017, pp. 1126–1135.

[31] A. Nichol and J. Schulman, "Reptile: A scalable metalearning algorithm," *arXiv preprint arXiv:1803.02999*, vol. 2, no. 3, p. 4, 2018.

[32] A. Rajeswaran, C. Finn, S. M. Kakade, and S. Levine, "Meta-learning with implicit gradients," *Advances in neural information processing systems*, vol. 32, 2019.